ULTRASONIC CHARACTERIZATION OF MICROSPHERICAL INCLUSIONS IN ZIRCONIA AND CRYSTALLIZED GLASS

A. Stockman and P.S. Nicholson

Ceramic Engineering Research Group
McMaster University
Hamilton, Ontario, Canada

INTRODUCTION

In high performance ceramic materials the critical flaw size is $\simeq 10\,\mu m$. Not all inclusions are equally detrimental to the structural properties. Therefore it is necessary to determine their size and composition.

The high frequency stress waves, (>10 MHz), produced by ultrasonic transducers are sensitive to changes of density and elastic modulus. In this work a mathematical model has been developed which calculates the waveforms and frequency spectra for sound waves scattered from various sized inhomogeneities as a function of the host and inclusion material parameters and the spectrum of the incoming sound waves.

The model is based on the work of Ying and Truell [1] (planar longitudinal waves incident on a spherical particle) but, to use the technique of ultrasound for defect detection, it is necessary to modify the analysis to incorporate the use of a focussed sound beam to increase the power and a pulsed system for locating of the defect.

To test the model spherical and near spherical voids in a glass matrix were first examined. Next spherical particles of oxides were embedded in the glass and the model compared with experiment. The glass was subsequently crystallized to approximate a real ceramic. Recently, spherical particles of platinum (50 and 200 μm diameter) have been embedded in dense zirconia. This work is reported. These inclusions were located ultrasonically by immersion scanning with a pulsed, focussed 25 MHz transducer. The backscattered signals were compared with the model predictions.

THEORY

Whereas the calculations of Ying and Truell [1] were performed to determine the total scattered energy from a spherical inhomgeneity [2], the equations can be used to calculate the amplitudes of the scattered waveforms from the inhomogeneity. The pressure experienced by the transducer which produced the initial sound wave is:

$$p(k) = P_{max}\, k\, a \frac{1}{\sqrt{2}} (1 + i) \exp[-ikz] \sum_{m=0}^{\infty} (2m + 1) A_m \qquad (1)$$

where $p(k)$ is the pressure for the wavenumber $k = 2\pi/\lambda$ (λ is the wavelength related to the frequency, f, and the longitudinal sound velocity, v_ℓ, as $= v_\ell/f$). P_{max} is the maximum pressure of

the wave at the site of the inhomogeneity. The distance from the transducer to the inclusion is z. The radius of the defect is a and A_m are the scattering amplitudes calculated using Ying and Truell with corrections of Gubernatis et al. [3]. These scattering amplitudes are functions of the density and shear and longitudinal sound velocities of the host and inclusion.

To include the effect of focussing the sound beam, the inhomogeneity is assumed to lie in the focal plane of the transducer and the equations developed by O'Neil [4] for the sound field of a focussed radiator expanded in a series expansion about the focal point to produce a modification to the wavenumber of;

$$k' = k\left(\frac{1+[1+(D/A)^2]^{1/2}}{2}\right) \tag{2}$$

where D is the diameter of the transducer and A is its radius. The quantity z in equation 1 is now the distance from the focal point of the transducer. This approximation limits the validity of the model to spheres < 200 μm diameter

The use of a pulsed sound beam instead of a continuous wave is accounted for by using a Fourier expansion of the incoming beam [5]. The reflected sound pulse from a flat surface in the focal zone of the transducer is transformed to yield the frequency composition of the incoming pulse. This is applied to Equation 1 to yield the pressure at the transducer as a function of frequency for a given inclusion radius. Figure 1 is the waveform (1(a)) of a signal reflected from a flat surface and its magnitude spectrum (1(b)). To simplify the calculations, the spectrum is approximated by a Gaussian distribution which can be described by its frequency at maximum amplitude (FMA) and its full width at half maximum amplitude (FWHM) (Figure 2). Using this approximation, the equation for the pressure at the transducer is given by:

$$P_T(f) = \frac{V_\ell a}{2\pi}\exp\left[\frac{-V_\ell}{2\pi f}Z\right]\exp\left[-4\ln 2\left(\frac{f-f_a}{f_{FWHM}}\right)^2\right]\sum_{m=0}^{\infty}(2m+1)A_m \tag{3}$$

where f_a is the FMA and f_{FWHM} is the FWHM.

Computer programs calculate the complex A_m values and these are then used to determine the spectra and waveforms. These spectra are then processed to calculate the FMA and FWHM. Inputted are the densities of the host matrix and the particles and their shear and longitudinal sound velocities. These were determined by direct measurement (especially for the zirconia matrix). The platinum parameters were taken from published values [6]. Table I shows the values used in the calculations. The FMA and FWHM of the incoming signal were also determined experimentally. Figures 3 and 4 are derived from the calculated values with straight lines joining the points. Some experimental values are also included in these figures. These programs do not use the amplitude of the calculated signals due to the varying attenuation factors between the measured values as the transducer height is changed for focussing The relative amplitudes of the frequency components do not change significantly.

EXPERIMENTAL

Particles of platinum were produced by melting pieces of Pt mesh in a crucible. The particles (diameter 50 to 120 μm) (approximately spherical) were laid in partially-stabilized zirconia (PSZ) powder within a locating ring of platinum, one particle per sample. Pellets were iso-pressed and fired to produce a dense body. The fired samples were ground and polished parallel. The inclusions were >4 mm deep in the PSZ. The density and longitudinal and shear sound velocities of the sample were measured.

The samples were immersion-scanned in H_2O with a 25 MHz focussed, pulsed transducer using a shock excitation system. This is a commercial test except the resolution of the scanning axis is 0.02 mm and the stepping axis is 0.01 mm. A computer controlled the scanner and recorded the amplitude of the signal during scanning. The computer also recorded the digitized waveforms, performed the Fourier transformations and analyzed the resultant spectra.

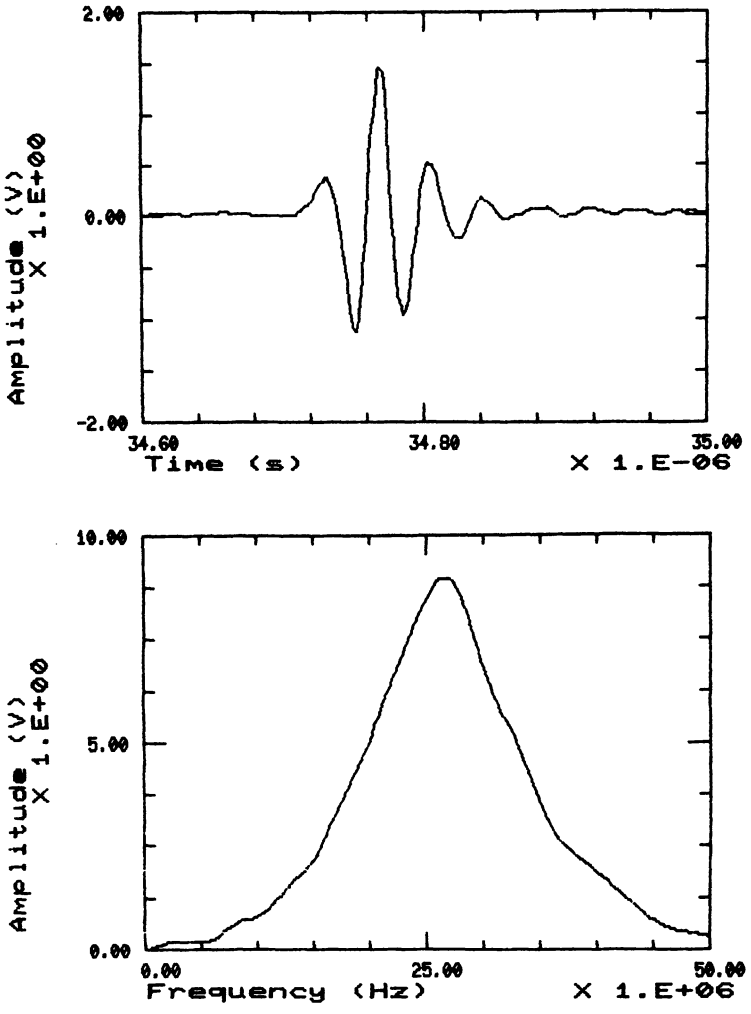

Fig. 1 Waveform and Spectrum of a sound pulse reflected from a flat surface at the focal zone of the 25 MHz focus, pulsed transducer.

The samples were scanned to locate the platinum locating ring (Figure 5) (darker regions indicate the higher amplitude signals). The ring can clearly be seen with a dark area in its center. This is the particle. The sample was cut and polished to the ring after the experiment and examined optically (Figure 6).

After location, the transducer height was adjusted to give the maximum signal amplitude from the inclusion. This was taken to correspond with the focal zone of the transducer. The signals were recorded, Fourier transformed and the FMA and FWHM measured by interpolation between points near the peak and at the half maximum amplitude locations. The measured values for 50, 65, and 100 μm diameter inclusions are shown in Figures 3 and 4 (large asterisks indicate the approximate error in measurements).

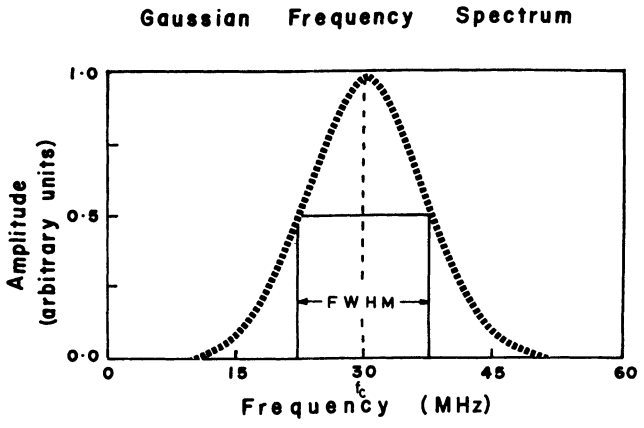

Fig. 2 Example of a Gaussian distribution showing the defining parameters FMA and FWHM.

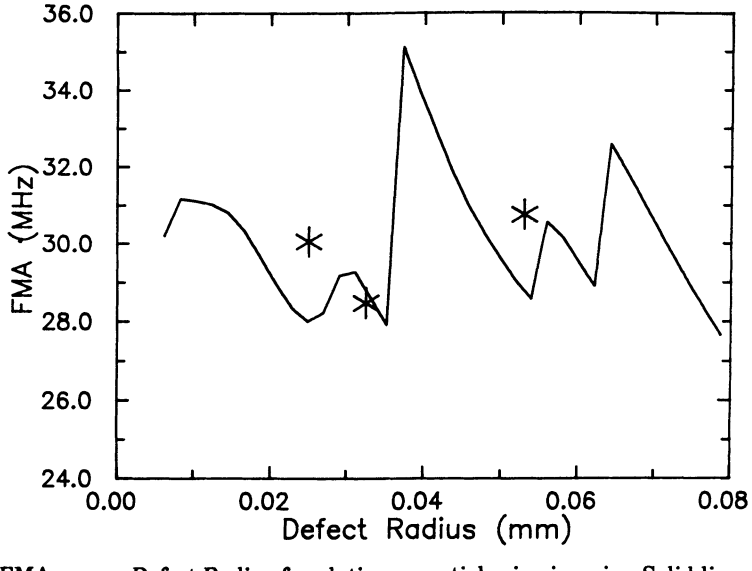

Fig. 3 FMA versus Defect Radius for platinum particles in zirconia. Solid lines are derived from theory and asterisks are data points and error estimates.

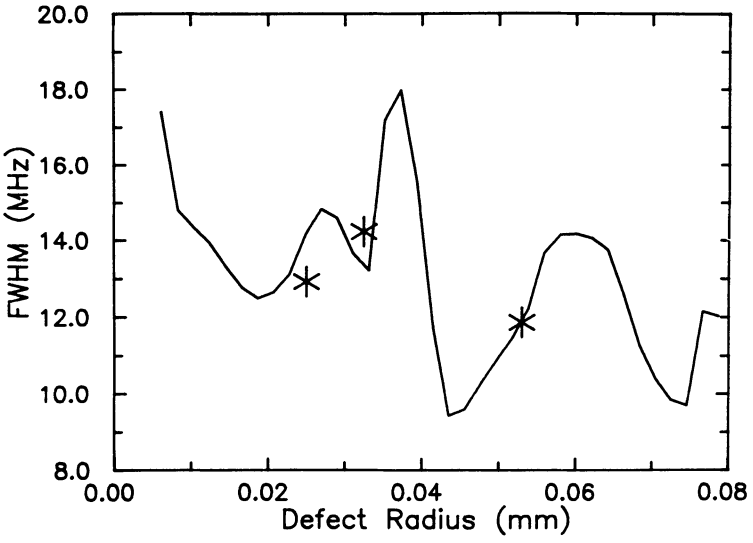

Fig. 4 FWHM versus Defect Radius for platinum particles in zirconia. Solid lines are derived from theory and asterisks are data points and error estimates.

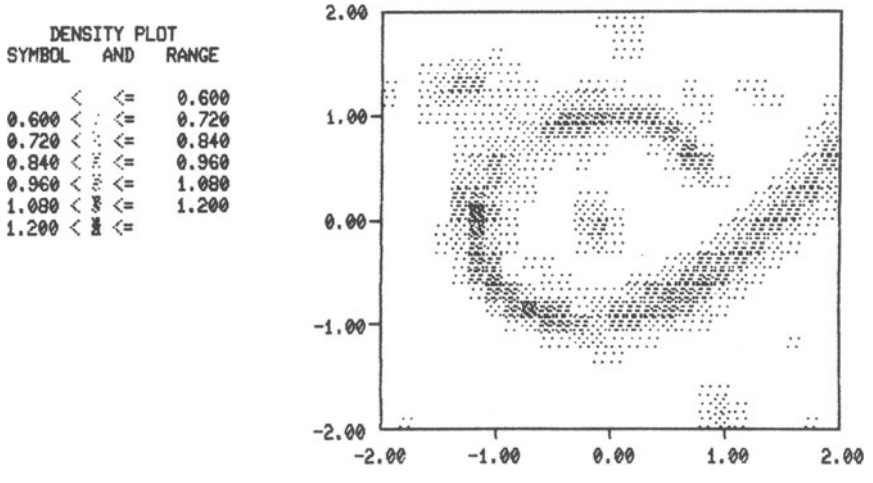

Fig. 5 Density plot of an ultrasonic scan of a zirconia sample with platinum ring and inclusion within. Darker regions represent higher amplitudes.

DISCUSSION

The measured values of FMA and FWHM for the 65 and 100 μm platinum spheres fit reasonably well with the theory (Figures 3 and 4). Minor variations will be due to the use of book values for Pt density and velocities. The accuracy of the measure of the 50 μm particle is in doubt due to its sticking to the crucible during manufacture. In fact it is possible that this particle became smaller during sample-sintering and surface tension may have drawn its rough sides into a sphere. Nevertheless its initial-measured value is plotted. The sample has not yet been cut and polished to the inclusion.

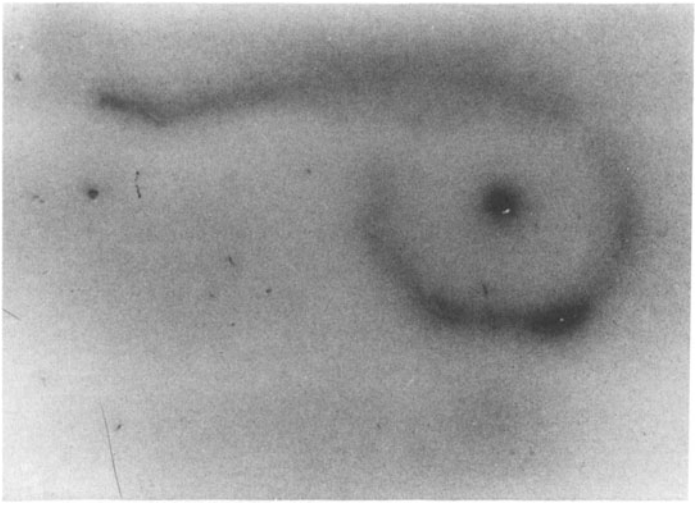

Fig. 6 Zirconia sample after cutting and polishing to expose the platinum ring and a 100 μm inclusion.

The discontinuous nature of FMA and FWHM curves is explained by resonances of certain component wavelengths of the incoming wave with the diameter of the inclusion [8]. Franz waves circumnavigate the inclusion (produced by the interaction of the incoming waves with the sphere) and are functions of the inclusion and host matrix material parameters. These Franz waves are not generally observable (due to their highly attenuated nature) in situations where the product of the wavenumber and inhomogeneity radius exceeds unity. The existence of these resonances is demonstrated by examining the waveforms and spectra for the 65 μm and 100 μm inclusions (Figures 7 and 8 - the model-predicted waveforms and spectra are shown in Figures 9 and 10). A tailing section (like a ringing of the signal) follows the main signal in the 100 μm inclusion waveform. The 65 μm waveform signal ends abruptly after the main pulse. The 100 μm "tail" is the result of a Franz wave and it produces two nearly-equal height peaks on the spectrum. The higher frequency peak is slightly higher. Had the inclusion been slightly smaller the first peak might have been larger so the FMA would shift sharply from the higher to the lower frequency. These resonances also produce shifts in the FWHM curves. The 65 μm inclusion spectrum exhibits a slight asymmetry on the higher frequency side (easily seen in the model spectrum). This too is attributable to a Franz wave albeit a much smaller effect.

Comparing the platinum-in-zirconia curves with the zirconia-in-glass and magnesia-in-glass curves (Figure 11) shows that the platinum particles exhibit a greater tendency to have resonances than do the zirconia particles. This could be due to the similarity of the zirconia shear velocity and the platinum longitudinal velocity and the strength of the resonance may be due to the density differences (see Table I). Zirconia and glass are more closely matched in longitudinal sound velocities and show only one strong resonance. Magnesia has a longitudinal velocity similar to the glass shear velocity and shows several weak resonances [9]. This point remains to be studied.

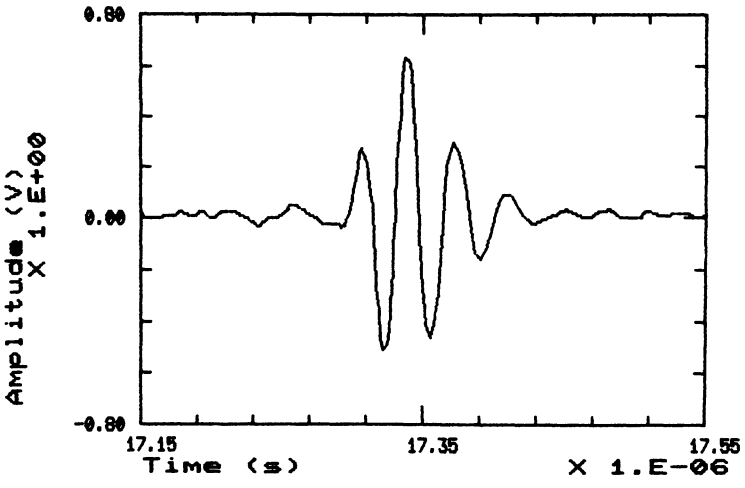

Fig. 7a Waveform and Spectrum from a 100 μm inclusion of platinum in zirconia.

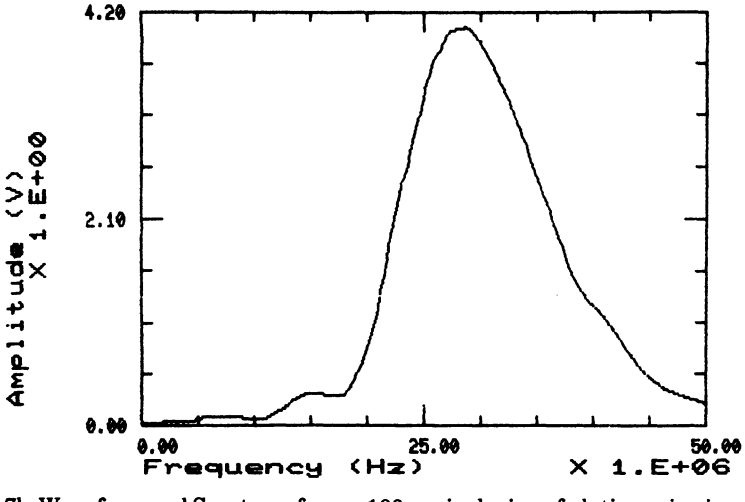

Fig. 7b Waveform and Spectrum from a 100 μm inclusion of platinum in zirconia.

CONCLUSIONS

Microspherical particles of platinum embedded >4 mm deep in a matrix of fine-grained zirconia were clearly visible using pulsed and focussed 25 MHz ultrasound. No grain-boundary effects interfered with the experiment. The model developed to understand the scattering of ultrasound from inclusions within a pulsed and focussed sound field was found to fit well with the experimental data with respect to predicting defect size.

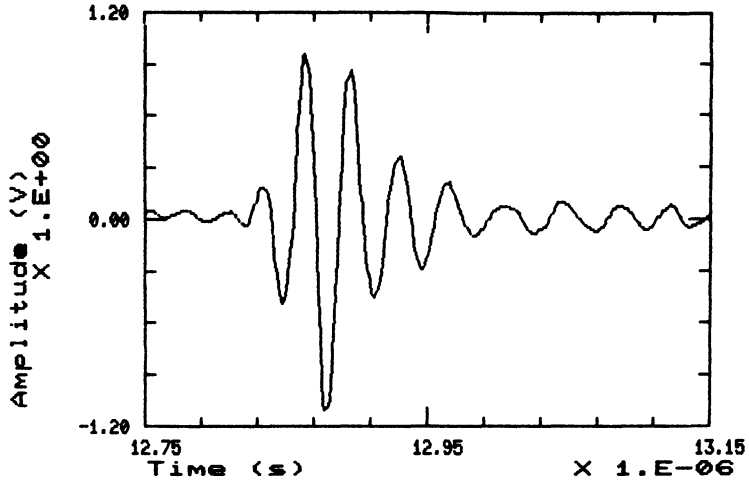

Fig. 8a Waveform and Spectrum from a 65 μm inclusion of platinum in zirconia.

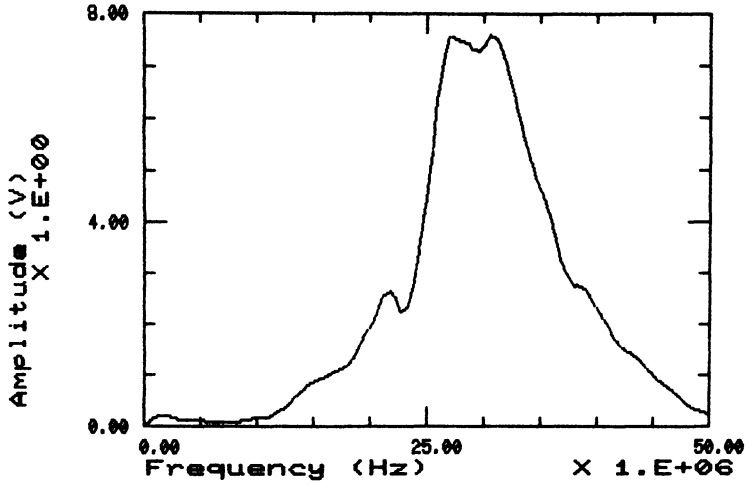

Fig. 8b Waveform and Spectrum from a 65 μm inclusion of platinum in zirconia.

ACKNOWLEDGEMENT

The authors wish to thank P. Sarkar for his invaluable assistance in producing the platinum particles and embedding them in the zirconia. J. van den Andel and N. D. Patel are acknowledged for their help in the experiments and discussions.

This work was funded by the Defence Research Establishment-Pacific, Victoria, British Columbia, Canada. (W. Starrock Scientific Authority).

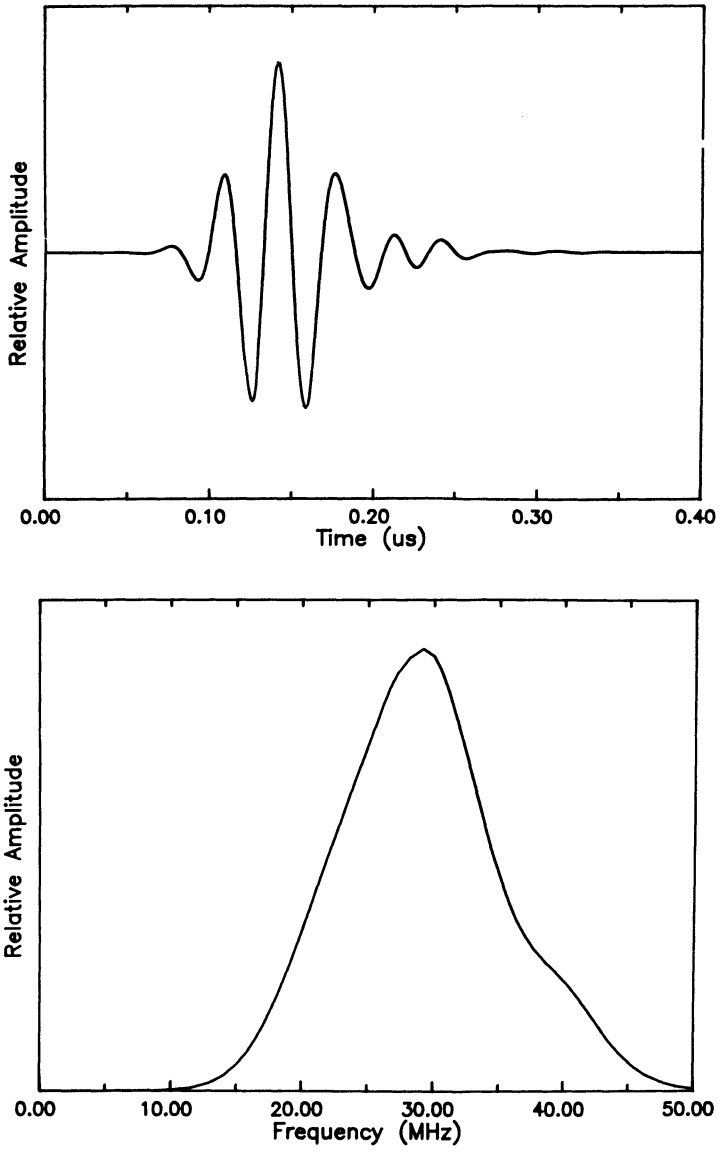

Fig. 9. Calculated waveform and spectrum for a 66 μm inclusion of platinum in zirconia

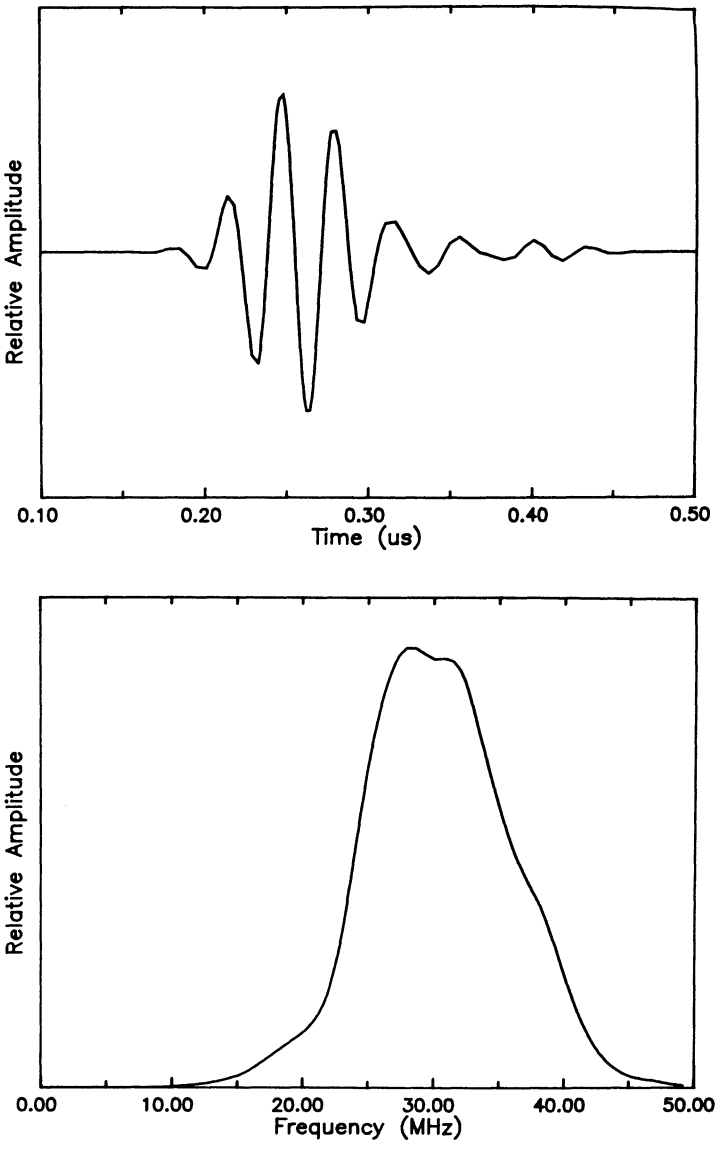

Fig. 10 Calculated waveform and spectrum for a 105 μm inclusion of platinum in zirconia.

TABLE I

Sonic and Material Parameters

Material	Density kg/m**3	Longitudinal Velocity m/s	Shear Velocity m/s
Zirconia	5900.	6927.	3654.
Platinum	21400.	3260.	1734.

Centre freq. (MHz) = 26.60 FWHM freq. (MHz) = 14.70

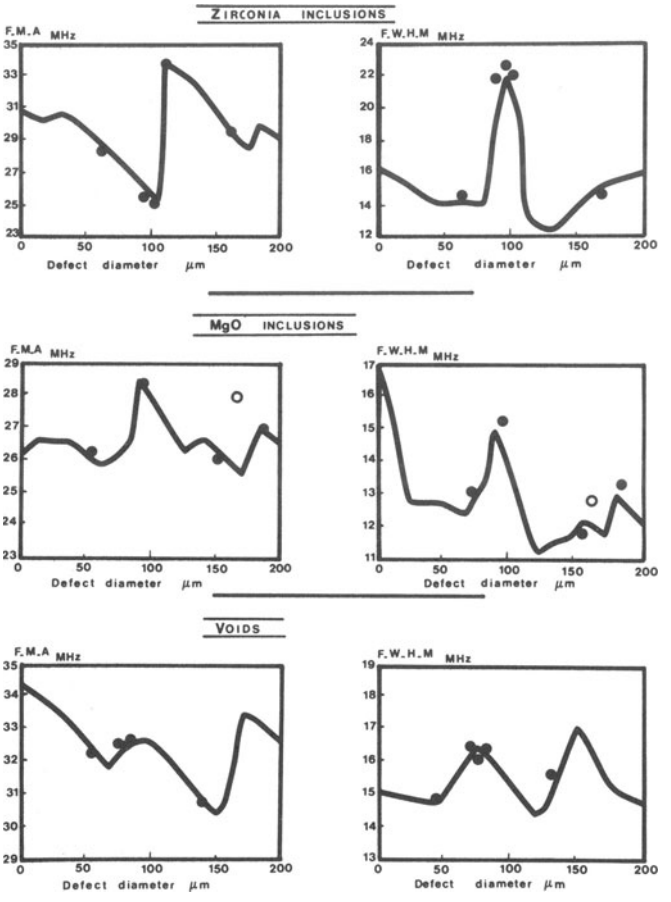

Fig. 11 FMA vs Defect Diameter and FWHM vs Defect Diameter for: 1) zirconia particles in F-glass, 2) magnesia particles in P-glass, and, 3) voids in crown glass.

REFERENCES

1. Ying C.F. and Truell R., "Scattering of a Plane Longitudinal Wave by a Spherical Obstacle in an Isotropically Elastic Solid", J. Appl. Phys., 27, 1956, pp 1086-1097.
2. Nicholson, P.S., "A Pedagogical Development of the Ultrasonic Characterization of Flaws in Advanced Ceramics" (this volume).
3. Johnson G. and Truell R., "Numerical Computation of Elastic Scattering Cross Section", J. Appl. Phys., 36, 1965, pp 3466-3475.
4. Gubernatis J.E., Domany E., Krumhansel J.A., and Huberman M., "The Born Approximation in the Scattering Elastic Waves by Flaws", J. Appl. Phys., 48, 1977, pp 2812-2819.
5. O'Neil H.T., "Theory of Focusing Radiators", J. Acoust. Soc. Am., 21, 1949, pp 516-526.
6. Tittman B.R., Cohen R.E., and Richardson J.M., "Scattering of Longitudinal Waves Incident on a Spherical Cavity in a Solid", J. Acoust. Soc. Am., 63, 1978, pp 68-74.
7. Handbook of Chemistry and Physics, 59th edition, (Chemical Rubber Company press, West Palm Beach Florida, 1978), p E-47.
8. Gaunaurd G.G., Tanglis E., Uberall H., Brill D., "Interior and Exterior Resonances in Acoustic Scattering I - Spherical Targets", Il Nouvo Cimento, 76B, 1983, pp 153-175.
9. Stockman A., Mathieu P., and Nicholson P.S., "Ultrasonic Characterization of Model Defects in Ceramics (Part 2): Spherical Oxide Inclusions in Glass - Theory and Practice", Materials Evaluation, 45, 1987, pp736-742.